Bennett, and E. J. Ashley, Phys. Rev. B **2**, 397 (1970).
[36]G. Wiech, in *Soft X-Ray Band Spectra and the Electronic Structure of Metals and Materials*, edited by D. J. Fabian (Academic, New York, 1968), p. 59; also G. Wiech and E. Zöpf, in Proceedings of the International Conference on Band Structure Spectroscopy of Metals and Alloys, Strathclyde, Sept., 1971 (unpublished).
[37]F. C. Brown and Om P. Rustgi, Phys. Rev. Lett. **28**, 497 (1972).
[38]D. E. Eastman and W. D. Grobman, in Proceedings of the Eleventh International Conference on the Physics of Semiconductors, Warsaw. These results are corroborated by recent data for Ge obtained using ESCA. See, L. Ley, S. Kowalczyk, R. Pollak, and D. P. Shirley, Phys. Rev. Lett. **29**, 1088 (1972).
[39]S. Kirkpatrick (private communication).
[40]J. P. Van Dyke, Phys. Rev. B **5**, 4206 (1972).
[41]J. D. Joannopoulis and M. L. Cohen, Solid State Commun. **11**, 549 (1972).

PHYSICAL REVIEW B VOLUME 7, NUMBER 8 15 APRIL 1973

Dispersion of Raman Cross Section in CdS and ZnO over a Wide Energy Range

R. H. Callender*
Physics Department, City College, City University of New York, New York 10031

S. S. Sussman,† M. Selders,‡ and R. K. Chang
Department of Engineering and Applied Science,§ Yale University, New Haven, Connecticut 06520
(Received 21 September 1972)

The dispersion of the Raman cross sections of several phonon modes in CdS and ZnO using a wide range of laser energies has been measured. The E_1(LO) and multi-LO (2-LO, 3-LO and 4-LO) modes in CdS have been studied over the energy range extending from $0.45E_{ex}$ (exciton energy) to $1.1E_{ex}$. For the E_1(LO) mode, both the "forbidden" (zz) and allowed (zx) geometries were employed. The dispersive behavior of the cross section in these two geometries is in agreement with theory for energies below E_{ex}. The dispersion of multi-LO-phonon scattering is also presented. For ZnO, the dispersion of the cross section for the E_1(LO), E_1(TO), A_1(TO), and E_2 modes was measured over the energy range of $(0.57\text{–}0.76)E_{ex}$. The behavior of the LO modes is expalined in terms of a cancellation between the deformation and Fröhlich contributions to the LO scattering cross section. For the TO modes, resonant cancellation was not observed, in contrast to the results of recent studies of CdS and ZnS. A simple model is used to discuss these differences between the ZnO and CdS behavior. Finally, a resonant enhancement of the scattering from the 2-LO mode in ZnO when the scattered-photon energy was coincident with E_{ex} is reported.

I. INTRODUCTION

Resonant Raman effects (RRE) in CdS have been extensively investigated both experimentally[1–11] and theoretically.[12–28] Much of the recent interest has centered on the dispersion of the allowed longitudinal-optic (LO), the "forbidden" LO, and the multi-LO modes. With laser photon energies $\hbar\omega_l$ below and near the exciton energy E_{ex}, the dispersion of the transverse optic (TO), allowed 1-LO, and 2-LO modes have been reported in several studies.[1,3,6–8,10,11,21] For $\hbar\omega_l > E_{ex}$, the data on the dispersive behavior of the allowed and forbidden 1-LO modes,[3,8,21] as well as the multi-LO modes, are very limited. For the 1-LO data, a particular problem with some of the previous results is that the polarizations of the input and scattered radiation were not always specified and, therefore, the separation between the allowed and forbidden 1-LO scattered intensities was in general not made.[5,21] This is partly because it has been only recently realized that the forbidden 1-LO intensity can be greater than the allowed 1-LO intensity for $\hbar\omega_l \simeq E_{ex}$.[4,10,22,23,27,29] In the case of the multi-LO dispersive behavior, only the resonant enhancement of the Raman intensity when the scattered-photon energy is nearly coincident with E_{ex} has been reported.[4,5]

For CdS at 80 °K, this paper presents the dispersion of the cross sections for the allowed 1-LO, forbidden 1-LO, and multi-LO (2-LO, 3-LO, and 4-LO) modes over a wide energy range of $\hbar\omega_l$ (from $\hbar\omega_l = 0.45E_{ex}$ to $1.1E_{ex}$). The data presented here make a substantial contribution to those already available in that (i) they were taken on the same crystal over a wider energy range; (ii) the scattering cross sections were corrected for the wavelength dependence of the instruments as well as for the reflection and absorption of the crystal—absorption measurements on the same crystal were used for these corrections; (iii) the scattering cross sections were normalized to the same CaF_2 crystal, which is assumed to exhibit only ω^4 dispersion; (iv) the scattering geometries were chosen such that the allowed and forbidden 1-LO and multi-LO modes would be observed and

uniquely identified. Therefore, we believe that these results will be useful in extending present theoretical work on RRE.

We have observed an enhancement of about four orders of magnitude for the allowed 1-LO cross section, compared with five orders for the forbidden 1-LO cross section as $\hbar\omega_l$ approached to within a 1-LO phonon energy from $E_{ex}(E_{ex}-\hbar\omega_l \simeq \hbar\omega_{LO})$. For $\hbar\omega_l$ above E_{ex} and increasing $\hbar\omega_l$, the decrease of the cross sections for the forbidden 1-LO and the multi-LO (2-LO, 3-LO, and 4-LO) modes was less steep than the enhancement observed as $\hbar\omega_l$ approached E_{ex} from below. The allowed 1-LO cross section, however, was about a factor of 10 smaller than that for the forbidden 1-LO when $\hbar\omega_l > E_{ex}$ and appeared to be decreasing more rapidly for increasing $\hbar\omega_l$. This latter behavior is in better agreement with theoretical calculations than was previous data,[21] in which the separation into allowed and forbidden components was not made.

The dispersion of the ZnO scattering cross section over a wide wavelength range has not been previously experimentally investigated. Only the dispersion of the 2-LO cross section has been measured from $E_{ex}-\hbar\omega_l = 1.4\hbar\omega_{LO}$ to $0.4\hbar\omega_{LO}$ by using a tunable dye laser.[11] The comparison between the dispersions of all the phonon modes in ZnO to those in CdS should be informative. Contrasted with CdS and other wurtzite-structure semiconductors, ZnO is particularly interesting because of its inverted valence-band structure[30] as a consequence of the admixture of the "d wave functions" of Zn. Like CdS and ZnS, ZnO has a large polaron coupling.[31] However, the spin-orbit splitting of ZnO is smaller and negative[30] compared to these crystals. Thus, the fact that the physical parameters of ZnO have similarities and differences compared with those of CdS and ZnS suggests that it would be interesting to investigate the dispersion of the Raman scattering cross sections of ZnO over a wide photon-energy range, as has been done for CdS[6,7] and ZnS.[32,33]

CdS exhibited resonant cancellation for the A_1 (TO) and E_1 (TO)[6] and E_2[7] modes when $\hbar\omega_l \simeq 0.85E_{ex}$. Only the E_1 (TO) mode was investigated in ZnS,[32,33] and that also exhibited resonant cancellation when $\hbar\omega_l \simeq 0.46E_{ex}$. No resonant cancellation was observed for ZnSe (zinc blende with a larger spin-orbit splitting).[30] This led to the speculation[33] that the parameters of the valence band (spin-orbit and crystal-field splittings) may be important in resonant cancellation of the Raman scattering cross section for modes that only involve the deformation-potential interaction.[12]

For ZnO, we measured the dispersion of the Raman cross sections for one-phonon scattering from $\hbar\omega_l = 0.57E_{ex}$ to $0.76E_{ex}$. The dispersions of the E_2, A_1 (TO), and E_1 (TO) modes over and above the normal ω^4 dependence were small and not unexpected since $\hbar\omega_l$ was quite far from resonance. However, for the A_1 (LO) and E_1 (LO) modes, our results were surprising. The A_1 (LO) was not observed and was at least a factor of 10^{-2} weaker than the A_1 (TO). The dispersion of the E_1 (LO) was significantly greater than that for the E_2, A_1 (TO), and E_1 (TO) modes in the same wavelength range.

It is well known that there are two possible mechanisms for LO Raman scattering. One mechanism involves the short-range interaction between the lattice displacement and the electrons. This interaction is put in terms of a deformation potential[12] and is the main mechanism for TO Raman scattering. Another mechanism for LO Raman scattering involves the long-range interaction generated by the macroscopic electric field associated with the LO phonon. This is termed the Fröhlich interaction.[12,14] These two mechanisms may be of equal magnitude and can interfere constructively or destructively.[12] Also, their dispersive behavior near and far from resonance can be different. The deformation contribution, which gives rise to TO scattering, may have pronounced dispersion. In CdS and ZnS, for example, it has been proposed that the deformation contribution actually changes sign as $\hbar\omega_l$ approaches E_{ex} from below.[6,7,32,33] The Fröhlich contribution can be linked[34,35] to the nonlinear optical susceptibility χ^{NL} responsible for sum frequency generation. The dispersion and sign of χ^{NL} have recently been of active interest.[36-40] Our results on the extremely low A_1 (LO) scattering cross section in ZnO [in contrast with the easily observable A_1 (TO) scattering] and on the dispersive E_1 (LO) cross section will be attributed to the destructive interference between the deformation and Fröhlich contributions to the LO scattering. A more detailed discussion is given in Sec. IV B.

For ZnO, we have also investigated multi-LO phonon scattering when the photon energy due to scattering with the 2-LO mode ($\hbar\omega_l - \hbar\omega_{2\text{-LO}} = 3.390$ eV) was near the exciton energy ($E_{ex} = 3.378$ eV) and when E_{ex} is between $\hbar\omega_l - \hbar\omega_{1\text{-LO}}$ and $(\hbar\omega_l - \hbar\omega_{2\text{-LO}})$. A significant enhancement of the cross section was observed when $\hbar\omega_l - \hbar\omega_{2\text{-LO}} \simeq \hbar\omega_{ex}$. The only previous uv work on ZnO[41] had $\hbar\omega_{7\text{-LO}} \approx \hbar\omega_{ex}$. Resonant enhancement when there is a coincidence of the scattered photon energy with the exciton energy has been noted previously in ZnS,[30] ZnSe,[30] and CdS.[4,5]

II. EXPERIMENTAL

The incident photon energies used in this experiment were restricted to the emission wavelengths of the Nd:YAG, krypton, argon, and He-Cd lasers.

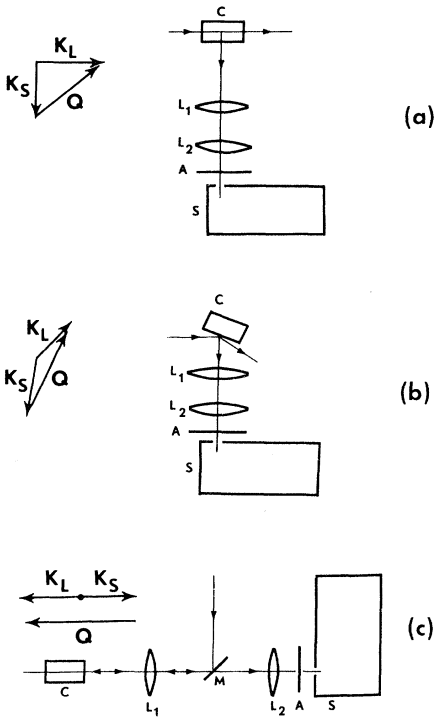

FIG. 1. Schematic drawing of the three geometries used: (a) shows a conventional right-angle geometry, (b) the reflection geometry, and (c) the backscattering geometry. In each case, C is the crystal (CdS, ZnO, or the CaF_2 reference crystal), L_1 is a collimating light-collecting lens, L_2 is a focusing lens, A is a polarizer, and S represents the spectrometer, phototube, and associated electronics. The vector triangle shows the propagation directions inside the crystal for each geometry. K_L, K_S, and Q are the laser light, Stokes signal, and phonon wave vector, respectively.

Three experimental scattering geometries were employed, as shown in Fig. 1. The "transmission geometry" is shown in Fig. 1(a); this is a conventional right-angle Raman scattering arrangement and was used for laser-photon energies below the exciton gap ($\hbar\omega_l < E_{ex}$) for all of the CdS work and for many of the ZnO experiments. The "reflection geometry" of Fig. 1(b) was used for CdS when $\hbar\omega_l \gtrsim E_{ex}$. As shown by the wave-vector conservation triangle, the collected light for this configuration is approximately backscattered. The "backscattering geometry" of Fig. 1(c) was used for ZnO for $\hbar\omega_l > E_{ex}$ and for some of the experiments when $\hbar\omega_l < E_{ex}$.

The polarizations of the input and scattered light waves for the ZnO experiments were varied in order to measure the different symmetry modes.[42] For the CdS work, both in the transmission and reflection geometries, the input polarization was always parallel to the crystal c axis. To measure the forbidden 1-LO and multi-LO modes, both the transmission geometry with $x(zz)y$ and the reflection geometry with $\sim x(zz)\sim\bar{x}$ (where $\sim x$ indicates approximately the x direction) were used. The allowed 1-LO was measured also in both transmission and reflection geometries with $x(zx)y$ and $\sim x(zx)\sim\bar{x}$, respectively. After each measurement on the CdS and ZnO crystals (in whichever of the three scattering geometries was appropriate), a CaF_2 crystal was substituted and the right-angle scattering from the 322-cm^{-1} mode was measured. The purpose of this was to normalize, for the ω^4 law, the laser power of the various laser emissions, the spectrometer and the phototube response, the light-collection efficiency, etc.

To rule out the possibility that some of the forbidden 1-LO intensity was due to a large collection angle, the forbidden LO intensity relative to CaF_2 was measured using $f/11$ collection optics compared to the $f/1.2$ normally used. No change was observed, and thus we can safely claim that the observation of the forbidden 1-LO is not due to an ill-defined scattering geometry.

For the CdS and ZnO crystals, the measured intensities of the Raman scattered light were appropriately corrected so that reliable values of the relative scattering cross section were obtained. For our data on CdS, the predominant correction is that of crystal absorption for laser-photon energies near and exceeding the crystal's exciton energy. For this purpose, accurate absorption measurements were done on a 2-mm-thick CdS sample, which was cut from the same CdS crystal used in our experiment

The incorporation of the correction due to CdS crystal absorption and reflection as well as the normalization by CaF_2 must be done before the Raman scattering cross section as a function of wavelength can be determined. The scattering cross section S is defined by

$$\frac{dI_s}{dx} = SI_l\Omega\,, \tag{1}$$

where I is the intensity, Ω is the effective solid angle, and the subscripts s and l refer to the scattered Stokes signal and input laser, respectively. The integration of (1), which yields the scattered Raman intensity, must take into account surface reflection and crystal absorption for both laser and scattered radiations in the appropriate manner for both the transmission and reflection geometries.

The results of this integration and a similar one for the CaF_2 reference crystal lead to the following expression for the transmission geometry:

$$\frac{S_{n\text{-LO}}^{CdS}}{S^{CaF_2}} = \left(\frac{I_{n\text{-LO}}^{CdS}}{I_s^{CaF_2}}\right)\alpha_l^{CdS}\, t^{CaF_2}\,\frac{(1-R_l^{CaF_2})(1-R_s^{CaF_2})}{(1-R_l^{CdS})(1-R_{n\text{-LO}}^{CdS})} \times \frac{\exp[(\alpha d)_{n\text{-LO}}^{CdS}]}{1-\exp[-(\alpha_l t)^{CdS}]}\left(\frac{\eta_{n\text{-LO}}^{CdS}}{\eta_s^{CaF_2}}\right)^2. \tag{2}$$

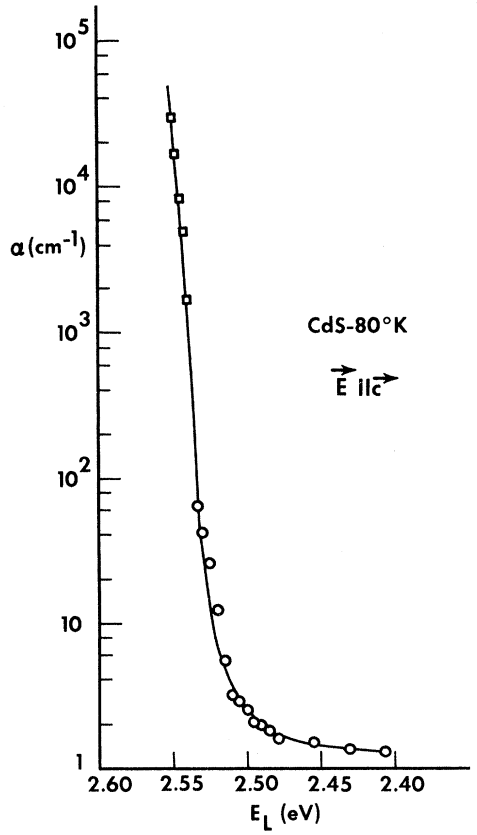

FIG. 2. Absorption of CdS for $\vec{E} \| \vec{C}$ at 80 °K. The circles are our measurements on a 2-mm-thick sample taken from the crystal used in these experiments; the squares are points taken from Ref. 43.

The subscripts l, s, and n-LO refer to the laser, Stokes signal in CaF_2, and (n-LO)th Raman signal in CdS, respectively. I is the measured intensity, α is the absorption coefficient, t is the crystal length (as limited by the collection-optics magnification and the spectrometer-slit height), R is the surface reflectivity, η is the index of refraction, and d is the distance in the CdS crystal traversed by the right-angle-scattered Raman signal.

For the transmission geometry with negligible loss at both laser and Raman-signal frequencies, Eq. (2) reduces to

$$\frac{S^{CdS}_{n\text{-LO}}}{S^{CaF_2}} = \frac{I^{CdS}_{n\text{-LO}}}{I^{CaF_2}_{s}} \frac{(1-R_l^{CaF_2})(1-R_S^{CaF_2})}{(1-R_l^{CdS})(1-R^{CdS}_{n\text{-LO}})} \times\left(\frac{\eta^{CdS}_{n\text{-LO}}}{\eta^{CaF_2}_{s}}\right) \frac{t^{CaF_2}}{t^{CdS}} . \quad (3)$$

The result of the integration of Eq. (1) for the reflection geometry is the following equation:

$$\frac{S^{CdS}_{n\text{-LO}}}{S^{CaF_2}} = \frac{I^{CdS}_{n\text{-LO}}}{I^{CaF_2}_{s}} (\alpha_l^{CdS} + \alpha^{CdS}_{n\text{-LO}})\, t^{CaF_2} \frac{1}{(1-R_l^{CdS})} \times\frac{(1-R_l^{CaF_2})(1-R_s^{CaF_2})}{(1-R^{CdS}_{n\text{-LO}})\{1-\exp[-(\alpha_l^{CdS}+\alpha^{CdS}_{n\text{-LO}})t^{CdS}]\}} \left(\frac{\eta^{CdS}_{n\text{-LO}}}{\eta^{CaF_2}_{s}}\right), \quad (4)$$

where CaF_2 has been assumed to be lossless.

For the reflection geometry in particular, the most important correction factor, as shown in Eq. (4), is the crystal absorption. In order to obtain reliable values for the absorption "tail" ($\alpha \leq 50$ cm^{-1}), we performed absorption measurements on a 2-mm-thick CdS slice, cut from the same CdS crystal used in our experiments. The absorption results are shown in Fig. 2. Our data are compatible with previously published results[43] and, along with other measurements, [44] were used to obtain the cross sections. The values of refractive index and reflectivity were obtained from the literature. [45,46] For the reflection geometry, the input-laser and scattered-Raman propagation directions are not normal to the crystal surface, and this was properly taken into account in computing R_l and R_s. [47]

To check the validity of Eqs. (2) and (4) for the transmission geometry and reflection geometry, respectively, measurements using both arrangements were made at the laser energy where the crystal begins to absorb and where both techniques are therefore applicable. The results of these measurements were within 20% of each other, which is considered to be good agreement.

III. RESULTS

A. CdS Crystals

The dispersion of the forbidden 1-LO (E_1) and the multi-LO phonon scattering cross sections taken in the (zz) geometry at 80 °K (normalized to CaF_2) are given in Fig. 3. In addition, the allowed 1-LO (E_1) and the 2-LO cross sections were measured in the (zx) geometry. The ratios of these data to those shown in Fig. 3 are plotted in Fig. 4. The dispersion characteristics of the other one-phonon modes in CdS for $\hbar\omega_l < E_{ex}$ have been studied extensively in the past and are not repeated here. In fact, the crystal used in these investigations is the same as used in Ralston *et al.* [6] in their studies of the dispersion of A_1 (TO), E_1 (TO), and E_1 (LO) modes for $\hbar\omega_l < E_{ex}$. For $\hbar\omega_l > E_{ex}$, a search was made for the A_1 (TO) mode, which is allowed for $\sim x(zz)\sim\bar{x}$ configuration, and the E_1 (TO) mode, allowed in $\sim x(zx)\sim\bar{x}$ configuration. These modes were not found.

The linewidths of the allowed and forbidden 1-LO scattered lines were less than 3 cm^{-1}.

1. One Phonon

The most interesting features of the 1-LO scattering shown in Figs. 3 and 4 are (i) the forbidden 1-LO cross section is enhanced by five orders of

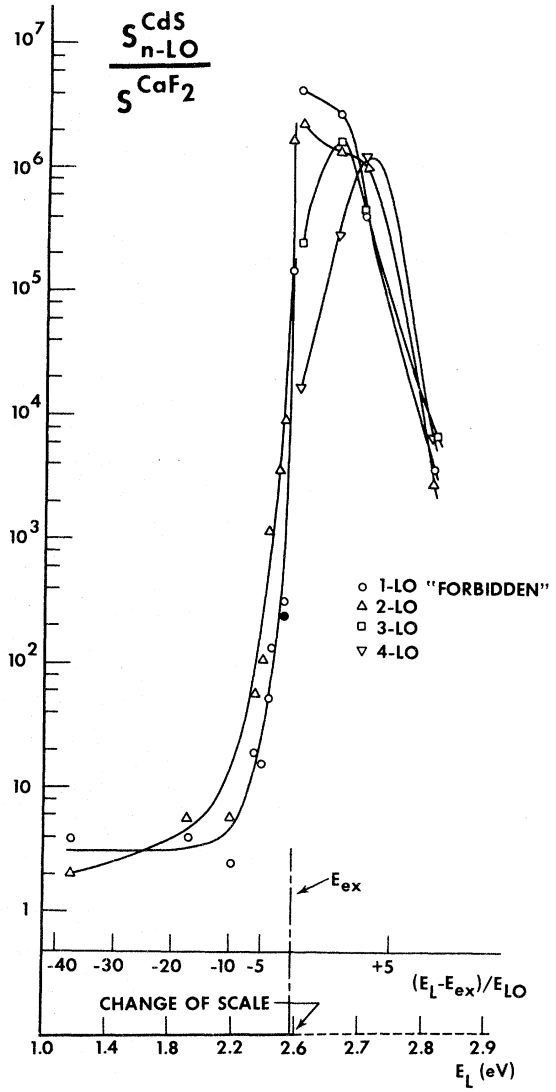

FIG. 3. Raman cross sections of CdS (80 °K), normalized to CaF_2, as a function of incident-photon energy. These data are from measurements taken in the (zz) geometry [i.e., $x(zz)y$ for $\hbar\omega_l < E_{ex}$ and $\sim x(zz) \sim \bar{x}$ for $\hbar\omega_l \gtrsim E_{ex}$]. In this geometry, the 1-LO scattering is "forbidden." The solid circle at 2.50 eV is the cross section measured in reflection, while the open circle above it was obtained in the transmission geometry. E_{ex} is the exciton gap energy for CdS. The upper abscissa scale shows the number of LO-phonon energies away from E_{ex}. Note the change of scale in the lower abscissa.

magnitude as $\hbar\omega_l$ approaches to approximately $E_{ex} - \hbar\omega_{LO}$ from below; (ii) the forbidden 1-LO cross section falls off by about two orders of magnitude for the range $\hbar\omega_l > E_{ex}$ shown; (iii) the forbidden 1-LO scattered intensity is still observable at $\hbar\omega_l = 0.45E_{ex}$; (iv) for $\hbar\omega_l < 2.40$ eV, the ratio of the allowed to forbidden 1-LO cross sections is approximately constant of a value of about 2; (v) for $\hbar\omega_l > 2.40$ eV, this ratio decreases monotonically by a factor of 20 over the measured range.

2. *Multiphonon*

The overtone (2-LO, 3-LO, 4-LO) scattering cross sections shown in Fig. 3 have the following features: (i) for $\hbar\omega_l < E_{ex}$, only 1-LO and 2-LO scattering was detectable. The 2-LO cross section has an enhancement of about six orders of magnitude as $\hbar\omega_l$ increases toward E_{ex}; (ii) for $\hbar\omega_l > E_{ex}$, many more overtones are observed

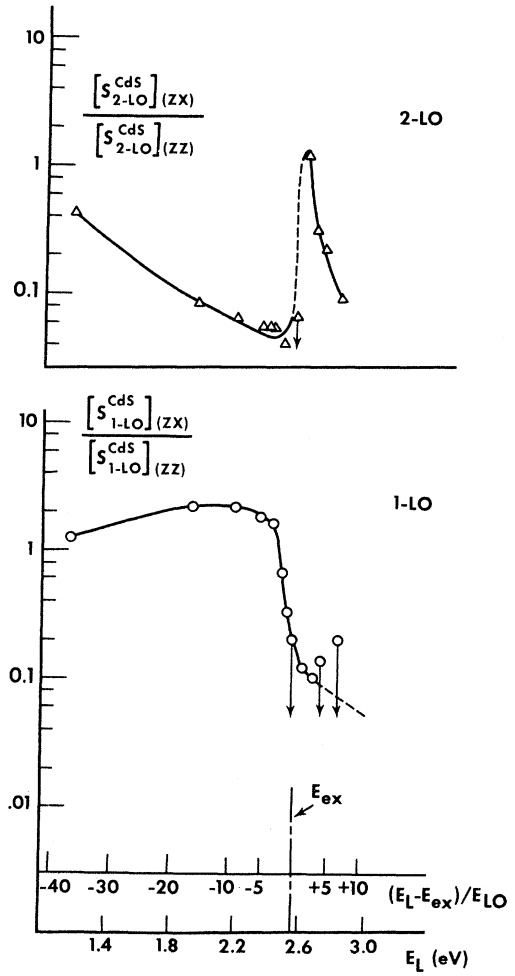

FIG. 4. Ratio of the cross sections measured in the (zx) geometry to those measured in the (zz) geometry for CdS (80 °K) as a function of incident-phonon energy. For the 1-LO scattering, this represents the ratio of the "allowed" to "forbidden" cross sections. The data points to which the descending arrows are attached represent upper limits of the ratio. The resolution of these points was limited by noise. The dashed portions of the curves are considered to be reasonable extrapolations. E_{ex} is the exciton gap energy for CdS. The upper abscissa scale shows the number of LO-phonon energies away from E_{ex}.

TABLE I. Relative intensity for multi-LO phonon scattering in ZnO (at 80 °K) for two different laser wavelengths (λ_l = 3507 and = 3564 Å). The intensities have been corrected for sample absorbtion, reflection, etc. (see text). The scattered intensities from one laser line are scaled arbitrarily with respect to the other laser line. The scattering configuration was $z(xx)\bar{z}+z(xy)\bar{z}$.

n-LO	Wavelength (Å)	Shift (cm^{-1})	Relative intensity	Linewidth[a] (cm^{-1})
		λ_l = 3507 Å		
1	3581	585	1	13.0
2	3658	1175	24	18.2
3	3738	1764	3	28.6
4	3821	2342	0.6	47.0
5	3912	2949	0.2	···
		λ_l = 3564 Å		
1	3640	585	10	13.0
2	3720	1175	20	18.2
3	3805	1764	3.0	28.6
4	3889	2342	0.6	49.5
		λ_{ex} = 3670 Å		

[a]The spectrometer linewidth of 5.2 cm^{-1} has been subtracted.

with a maximum of six overtones in our experiments, while eight overtones have been previously observed[4,5]; since only three overtones were observed over the entire range of laser energies, only three overtones were included in the figure; (iii) the 3-LO and 4-LO cross sections have peak values at an energy such that $\hbar\omega_l - E_{ex} \simeq E_{3\text{-LO}}$ and $E_{4\text{-LO}}$ respectively; (iv) for the 2-LO, as shown in Fig. 4, the ratio of the cross section measured in the (zx) geometry to that in the (zz) geometry decreases by an order of magnitude for $\hbar\omega_l$ approaching E_{ex} from below, appears to increase rapidly near E_{ex}, and then decreases again for $\hbar\omega_l > E_{ex}$. This apparent oscillatory behavior requires further investigation using a tunable laser. We believe that this paper is the first detailed presentation of the dispersion of the multiphonon cross section.

B. ZnO Crystal

1. One Phonon

Figure 5 shows the relative Raman cross section of the one-phonon scattering as a function of incident laser energy. The variations of the cross sections have been normalized to the 322-cm^{-1} mode of CaF_2, as explained previously. The cross sections shown are for the E_1 (zx) (LO), E_1 (zx) (TO), A_1 (xx) (TO), A_1 (zz) (TO), and the E_2 (xx) modes. The cross sections for the various modes have been scaled by different factors to accent the dispersion characteristics, and thus absolute scattering cross sections are not obtainable from Fig. 5. The absolute Raman cross sections have been reported elsewhere[48] using 5145-Å radiation.

A search was made for the A_1 (xx) (LO) phonon. The cross section for the A_1 (xx) (LO) mode was not measurable by our apparatus and is less than 5×10^{-3} of that of the A_1 (xx) (TO) mode for all laser energies used. These ZnO data were all taken at room temperature.

2. Multiphonon

The multiphonon data for the two exciting laser lines of the krypton laser above the exciton energy of ZnO are tabulated in Table I. Shown for each line are the relevant multiphonon parameter, i.e., positions of the n-LO multiphonon peaks, relative intensity, and linewidth [full width at half-maximum (FWHM)]. The scattering configuration used was $z(xx)\bar{z}+z(xy)\bar{z}$ and the sample temperature was 80 °K. The intensities were corrected using procedures discussed in Sec. II. We used the absorption constant measured by Yoffe,[49] and

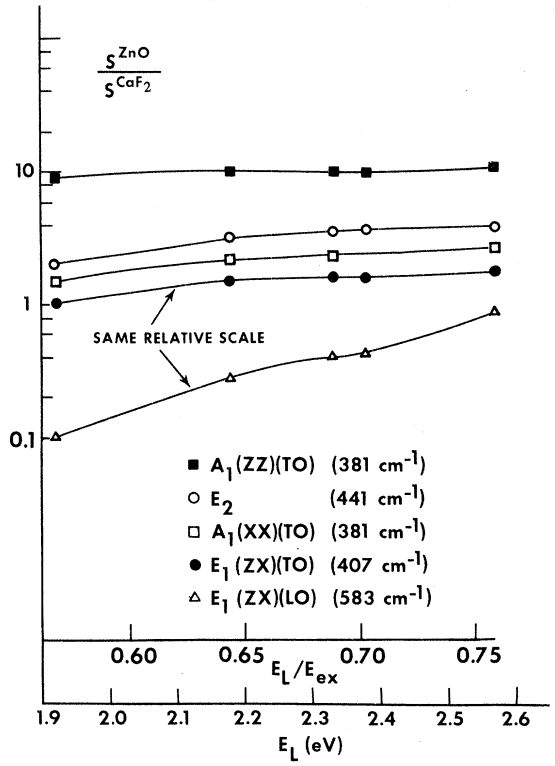

FIG. 5. Raman cross sections of ZnO (300 °K), normalized to CaF_2, as a function of incident-photon energy. The E_1 (zx) (TO) and E_1 (zx) (LO) cross sections are plotted on the same relative ordinate scale, while the other cross sections have been scaled by different factors to accent their dispersion characteristics. The upper abscissa scale shows the ratio of incident-laser energy (E_L) to that of the excition gap energy (E_{ex}).

the reflectivity measured by Thomas.[50] The relative intensities as given in Table I are fairly sensitive to reflectivity corrections. Due to variations in surface quality, Thomas has found that the reflectivity in ZnO can vary significantly. We estimate that the relative intensity ratios in Table I are accurate to within a factor of 2 chiefly because of this surface effect. Note that even with this ambiguity, the 2-LO phonon intensity when measured with a 350-Å laser line ($\hbar\omega_l - \hbar\omega_{2\text{-LO}} = 3.390$ eV, $E_{ex} = 3.378$ eV) shows a significant resonant enhancement. A search was made for TO scattering above the exciton gap in ZnO. As in the case of CdS, we did not observe any TO scattering for these two laser lines which are above the exciton energy.

IV. DISCUSSION

A. CdS Crystal

1. One Phonon

The dispersion of the cross sections of the TO modes with A_1 and E_1 symmetries has been previously reported by Ralston *et al.*[6] for $\hbar\omega_l < E_{ex}$. A pronounced decrease was observed prior to the onset of resonance enhancement as $\hbar\omega_l$ approached E_{ex} from below. In this paper, we note the disappearance of the scattered intensity for these TO modes for $\hbar\omega_l > E_{ex}$. This result remains unexplained, although this observation has been previously noted.[5]

The dispersion of the allowed 1-LO (E_1) cross section for $\hbar\omega_l < E_{ex}$ has previously been reported[6,7,21] and was found to increase monotonically as $\hbar\omega_l$ approached E_{ex} from below. In our investigation we have reconfirmed this observation (see Figs. 3 and 4). The data are in reasonable agreement with the theory for this energy range.[21,28] In addition, our data show a greater enhancement for the forbidden 1-LO cross section compared to the allowed 1-LO for $\hbar\omega_l$ below and very near E_{ex}. Quantitative comparison between these data and recent calculations[22,23,28] reveal excellent agreement in this region. However, we are aware of no theory that can explain the relatively large forbidden 1-LO cross section when $\hbar\omega_l$ is so far away from E_{ex} ($\hbar\omega_l \simeq 0.45E_{ex}$).

For $\hbar\omega_l > E_{ex}$, our results indicate that the forbidden 1-LO cross section decreases more slowly for increasing $\hbar\omega_l$ than the corresponding falloff for decreasing frequencies below E_{ex} (see Fig. 3). This does not agree with the theory for this energy region,[28] which is in the early stages of development. As shown in Fig. 4, the ratio of the allowed to forbidden 1-LO cross sections is decreasing, indicating that the allowed 1-LO cross section is decreasing faster than the forbidden one. Our data are in better agreement with the theoretical curve of Bendow *et al.*[21] than the experimental results presented in their paper. Martin and Damen[23] stated that the data of Ref. 21 were unpolarized. In that case, the unpolarized data of Ref. 21 would include intensities both from allowed and forbidden 1-LO scattering. We recall that Fig. 4 shows that the allowed cross section is decreasing faster than the forbidden cross section in this region. This explains why our measurements for the allowed 1-LO are in better agreement with the theoretical curve of Ref. 21, which is calculated only for allowed scattering. Before a more definitive statement can be made, further measurements of these cross sections should be made with a continuously tunable laser over as wide a range as possible, using properly selected polarizations for the input and scattered radiation. In addition, further theoretical effort on this problem, particularly for $\hbar\omega_l > E_{ex}$, is necessary.

2. Multiphonon

The dispersion of the 2-LO cross sections for the (zz) and (zx) geometries is shown in Figs. 3 and 4. Note that for the (zz) geometry, the 2-LO cross section is greater than the 1-LO cross section for $\hbar\omega_l \gtrsim 1.6$ eV. Figure 4 also indicates that except for $\hbar\omega_l$ very near E_{ex}, the 2-LO cross section for the (zz) geometry exceeds that for the (zx) geometry. The oscillatory behavior of Fig. 4 for $\hbar\omega_l \simeq E_{ex}$ requires confirmation with tunable lasers.[11]

For the (zz) geometry, the 3-LO and 4-LO cross sections have peak values when the scattered photon energy equals E_{ex}. Qualitatively such a peak can be explained by most existing theories as being due to a pole in the energy denominator of the calculated cross section when the scattered photon energy equals E_{ex}. Quantitative calculations for the dispersion of the cross section for the multi-LO phonon modes are not yet available.

B. ZnO Crystal

1. One Phonon

From the data given in Fig. 5 for $\hbar\omega_l < E_{ex}$, it is apparent that the E_2, A_1 (xx) (TO), A_1 (zz) (TO), and E_1 (zx) (TO) cross sections are relatively dispersionless in the wavelength range studied ($\hbar\omega_l \simeq 0.57E_{ex}$ to $0.76E_{ex}$). This should be contrasted with two other wurtzite materials, CdS[6,7] and ZnS,[8,9] where measurements on the TO dispersion showed a severe intensity variation in this analogous wavelength range. For ZnO, we can conclude that no resonant cancellations exist in a photon energy range comparable in terms of percentage of E_{ex} as contrasted with the case for CdS and ZnS.

The two most striking features in ZnO are the following: (i) The E_1 (LO) mode dispersion is

relatively large, and (ii) the $A_1(xx)$ (LO) mode is absent. In ZnS and CdS, however, the E_1 (LO) mode is fairly dispersionless in this range of $\hbar\omega_l/E_{ex}$, and the A_1 (xx) (LO) mode is quite large.[48]

In order to explain the above two striking features in ZnO, we consider the two scattering mechanisms for the Raman effect. Following Loudon[51] and Kaminow and Johnston[34] and using the latter's notation, the Raman cross section for the TO modes (S_T) and the LO modes (S_L) can be written as (ignoring plasmon and polariton effects)

$$S_{L,T} = \sigma_{L,T}\rho^{-1}\left|\frac{d\alpha_{12}}{dQ_3}\right|^2_{L,T} , \tag{5}$$

where

$$\sigma_{L,T} = \frac{\hbar\omega_s^4(N_{L,T}+1)\,t\,d\Omega}{32\pi^2\epsilon_0^2c^4\omega_{L,T}} , \tag{6}$$

with $\omega_{L,T}$ the LO or TO mode frequencies, ω_s the scattered frequency, ϵ_0 the permittivity of free space, $N_{L,T}$ the Bose population factor, t the scattering length, and ρ the reduced mass density. For the TO modes, $d\alpha_{12}/dQ_3$ contains only the deformation contribution. For the LO modes, the Fröhlich contribution also is present. Again, following Kaminow and Johnston, we can write for the TO modes

$$\left(\frac{d\alpha_{12}}{dQ_3}\right)_T = \alpha_{123} , \tag{7}$$

and for the LO modes

$$\left(\frac{d\alpha_{12}}{dQ_3}\right)_L = \alpha_{123} + \xi_{123}\left(\frac{m}{e^*}\right)(\omega_T^2-\omega_L^2) , \tag{8}$$

where e^* is the effective charge of the LO mode and m is the reduced mass of the vibration. In Eq. (8), α_{123} is the deformation contribution to the Raman amplitude, and $\xi_{123}(m/e^*)(\omega_T^2-\omega_L^2)$ is the Fröhlich contribution. In these equations we have neglected the effects of finite phonon lifetimes. The ξ_{123} can have three independent elements in the wurtzite crystals, namely, ξ_{zzz}, ξ_{xxz}, and ξ_{xzx} associated with the A_1 (zz) (LO), A_1 (xx) (LO), and E_1 (zx) (LO) phonons, respectively. As we have mentioned before, the deformation and Fröhlich contributions can either be additive or subtractive and can be of the same order of magnitude.

The very low intensity (if it exists at all) of the scattering from the A_1 (xx) (LO) phonon and the relatively large Raman intensity of the scattering from the A_1 (xx) (TO) phonon indicate that the deformation and Fröhlich contributions interfere destructively and, in fact, cancel each other. Since $S_L/S_T \leq 5\times10^{-3}$ in the region studied, we can calculate the ratio of the deformation to Fröhlich contributions for A_1 (xx) (LO) phonons. Using Eq. (8), we have $(\xi_{xxz}/\xi_{xxz})(m/e^*)(\omega_T^2-\omega_L^2) = -1$ to within ± 10%, where the error reflects the uncertainty in S_L/S_T. It is conventional to use a dimensionless parameter $\gamma_{123} = (\xi_{123}/\alpha_{123})(m/e^*)\omega_T^2$, which defines a ratio of the Fröhlich and the deformation contributions. For ZnO, the result is $\gamma_{xxz} = 0.76$ (± 10%). The other two independent values of γ for ZnO have been measured previously by Ushioda *et al.*[52,53] who found that $\gamma_{zzz} = 1.5$ and $\gamma_{xzx} = 1.4$ at $\hbar\omega_l = 1.97$ eV (6328 Å). For CdS, the three values of γ have been measured by Scott *et al.*[54] using polariton scattering at $\hbar\omega_l = 2.41$ eV (5145 Å). For ZnS, only the magnitude of one value of γ has been determined and the sign of that is still ambiguous.[52,53] Note that all of the three values of γ for ZnO and CdS are positive.[55]

A correspondence can be made between ξ_{123} and the second-harmonic-generation (SHG) coefficient d_{123}, namely, $\xi_{123} = 4\epsilon_0 d_{321}$, where ϵ_0 is the permittivity of free space.[34] Recently, the absolute signs of d_{321} have been determined in a variety of materials including CdS and ZnO.[37] It is possible to determine the absolute signs of the deformation and Fröhlich contributions to the Raman amplitude with a combination of Raman data and SHG data if the sign of the effective charge e^* is known.[56]

We will assume that $e^* < 0$ for CdS[57] and ZnO. In Table II, we have tabulated the signs of d reported by Miller and Nordland[37] and the signs of α which are consistent with the positive γ and the appropriate signs of the d coefficients. Note that in each case the signs for α_{123} for ZnO measured in our wavelength range are opposite to those of CdS determined at 2.41 eV (5145 Å). This is due to the reversal of the sign of the d coefficient in going from ZnO to CdS and the fact that γ_{123} is positive. This sign reversal of the d coefficient has been attributed to the influence of the d electrons, the influence being larger in ZnO than in CdS.[58]

We now examine the dispersive characteristic of α in CdS and ZnO. As mentioned above, the positive sign of γ for CdS was determined at 2.41 eV (5145 Å). Due to the resonant cancellation for

TABLE II. Sign of the second-harmonic-generation coefficient d and the deformation contribution to the Raman scattering amplitude α for CdS and ZnO. The sign of d is according to measurements reported in Ref. 37. The sign of α is deduced by assuming e^* to be negative for ZnO and CdS and by using the fact that γ are all positive for CdS at 5145 Å (Ref. 54) and ZnO (this work and Refs. 52 and 53). The sign of γ and thus α in CdS may change for $\lambda_l < 5400$ Å due to resonant cancellation of the TO mode (Ref. 6).

	α_{xxz}	d_{zxx} (d_{31})	α_{zzz}	d_{zzz} (d_{33})	α_{xzx}	d_{xzx} (d_{15})
ZnO	−	+	+	−	−	+
CdS	+	−	−	+	+	−

the TO modes,[6] the sign of α is presumed to change for energies below the cancellation-point energy [2.11 eV for the E_1 (zx) (TO) mode and 2.24 eV for the A_1 (zz) (TO) mode]. Let us take the simple model proposed by Ralston *et al.*[6] which suggests that $\alpha = Af(\omega_g - \omega_l) + B$. The $Af(\omega_g - \omega_l)$ term arises from the most resonant term using Loudon's free-electron-hole picture[12] applied to the conduction and valence bands, while the B term arises from higher bands and nonresonant terms from the conduction and valence bands. The numerical values of A and B are determined from a best fit to the experimental data. For resonant cancellation, the signs of A and B must be opposite since $f(\omega_g - \omega_l)$ is always positive for $\omega_l < \omega_g$. Ralston *et al.*[6] could determine only the relative signs of A and B. Using the values given in Table II, the absolute signs of these coefficients can now be determined.

Let us examine in detail the signs of A and B for the E_1 (zx) (TO) mode. For CdS at 2.41 eV (5145 Å), $Af(\omega_g - \omega_l)$ is the predominant term. In order to make α_{xzx} positive (see Table II) and account for resonant cancellation, it is required that $A > 0$ and $B < 0$. For ZnO, α_{xzx} is negative (see Table II). In addition, our experimental data (see Fig. 5) indicate that there is no resonant cancellation for the E_1 (zx) (TO) mode in ZnO. Therefore, we conclude that $A < 0$, $B < 0$, a reversal of the sign of A. Similar arguments can be applied to α_{zzz} [i.e., A_1 (zz) (TO) mode], where a sign reversal also occurs in going from CdS to ZnO. There was no resonant cancellation for the A_1 (zz) (TO) in ZnO, in contrast with CdS. Thus, for this A_1 (zz) (TO) mode in ZnO $A < 0$, $B < 0$, as was the case for the E_1 (zx) (TO) mode.

Since the role of the d electrons due to the Zn ions is to substantially change the valence-band structure of ZnO[59] as compared to CdS[30] (and is probably the reason for the inverted band structure of ZnO as compared to other wurtzites[30]), it is reasonable to suggest that a reversal of the sign of A in going from CdS to ZnO is also due to the effect of the d electrons. This suggestion supports the arguments of Lewis *et al.*[33] that cancellation effects may depend on the values of the spin-orbit and crystal-field coupling in these materials. The crystal-field splittings for ZnO and CdS are of comparable strength ($\Delta_{cr} = 0.027$ eV for CdS, $\Delta_{cr} = 0.04$ eV for ZnO). Due to the different mixing of the d electrons into the valence band, the spin-orbit splittings are very different ($\Delta_{so} = 0.065$ eV for CdS and $\Delta_{so} = -0.0047$ for ZnO).

Finally, we note that since γ_{xzx} is positive, the deformation and Fröhlich contributions to the E_1 (zx) (LO) scattering cross section are destructively interfering. Figure 5 shows that the E_1 (zx) (LO) mode has a smaller and more dispersive cross section than the E_1 (zx) (TO) mode. We believe that this is because the two contributions to the LO cross section have comparable magnitudes but opposite signs and somewhat different dispersive characteristics.

2. *Multiphonon*

The two available laser lines of the krypton laser lie in a fortuitous region with respect to the band properties of ZnO. One of the laser emissions ($\lambda_l = 3564$ Å) gives rise to Raman scattering such that the exciton peak of ZnO lies between the scattered frequencies at 1-LO and 2-LO; the other laser wavelength ($\lambda_l = 3507$ Å) produces Raman scattering at 2-LO (3.390 eV) which is nearly coincident with that of the exciton energy (3.378 eV).

The data shown in Table I have two interesting features. First, comparing the relative intensities of 1-LO and 2-LO for the two laser lines, a large enhancement of the 2-LO scattering is observed when the 2-LO scattered frequency is nearly coincident with the exciton frequency demonstrating a clear resonant enhancement. Second, we see that for both laser lines used the intensities for n-LO ($n > 2$) scale as the intensity of 2-LO, i.e., when 2-LO is enhanced n-LO ($n > 2$) is also enhanced by the same factor. Although theories of multi-LO Raman scattering have not been as yet well developed,[60] most theories do qualitatively predict this type of behavior. In general, these theories give a resonant enhancement whenever the incident light or scattered light is coincident with the exciton energy, $\hbar\omega_{ex}$. If the n-LO scattered-photon energy is coincident with $\hbar\omega_{ex}$, then all the m-LO ($m > n$) scattered efficiencies are correspondingly enhanced. Such theories are normally called "intermediate resonance theories." More detailed quantitative investigations of the dispersion characteristics of n-LO and comparison to theory need to await tunable dye lasers.[11]

V. CONCLUSION

From the data presented here, we make the following concluding remarks.

(i) The dispersion of the Raman cross section for the LO modes in CdS is at present treated only by theories over a relatively small energy range close to and below the exciton gap. Thus, our observation that the forbidden LO scattering is still strong for $\hbar\omega_l \ll E_{ex}$ is theoretically not yet explained; nor is our measurement on the strong forbidden LO scattering for $\hbar\omega_l > E_{ex}$ accountable by present calculations. Theories for this energy range have to take into consideration electronic transitions to higher bands and additional scattering mechanisms. Our present results in CdS have already stimulated such calculations.[61]

(ii) The ratio of the allowed to the forbidden

scattering in CdS changes very rapidly in the vicinity of the exciton gap. It should be interesting to study this behavior in more detail with a tunable dye laser.

(iii) The dispersion of the multi-LO phonon scattering is theoretically less developed than that for the 1-LO scattering. Even qualitative explanation of our dispersion data has to await further theoretical developments. However, existing theories do predict the enhancement of the cross section when the scattered-photon energy is equal to E_{ex}.

(iv) In ZnO, we have observed that the cross section for the A_1 (xx) (LO) mode is markedly smaller than that for the A_1 (xx) (TO) mode over a wide energy range. This was explained by the destructive interference of the deformation potential with the Fröhlich contribution. A similar mechanism was previously used to explain the unobserved E (LO) scattering in tellurium, when the laser photon energy was far above the exciton gap.[62] The dispersion of the E_1 (zx) (LO) mode and the extremely small A_1 (xx) (LO) cross section over such a wide energy range is not yet fully understood.

(v) We have found no resonant cancellation for the TO modes in ZnO, which is a wurtzite-structure crystal. This is to be contrasted with previous work on other wurtzite-structure crystals (CdS and ZnS) which reported observation of resonant cancellation. Earlier investigation on cubic-structure crystal (ZnSe) indicated no resonant cancellation of the TO cross section. We conclude that the cancellation of the scattering of the TO mode is not intrinsically related to the crystal structure but is due more to the specific electronic band structure. Further experimental investigations on crystals with cubic and wurtzite structure are in progress.

ACKNOWLEDGMENTS

We acknowledge the technical assistance of R. Fenstermacher (C. U. N. Y.) and P. B. Klein (Yale). Discussions with J. L. Birman and R. Zeyher (N. Y. U.) and C. Flytzanis (Harvard) have been helpful and we wish to thank them.

*Supported in part by the Air Force Office Of Scientific Research (AFOSR) under Grant No. 72-2209 and in part by the City University of New York Faculty Research Award Program.

†Present address: Lawrence Livermore Laboratory, P.O. Box 808, Livermore, Calif. 94550.

‡Fellow of the Deutsche Forschungsgemeinschaft.

§Supported in part by the Office of Naval Research Grant No. NOOO14-67-A-0097-0005.

[1]R. C. C. Leite and S. P. S. Porto, Phys. Rev. Lett. **17,** 10 (1966).

[2]J. F. Scott, R. C. C. Leite, and T. C. Damen, Phys. Rev. **188,** 1285 (1969).

[3]R. C. C. Leite, T. C. Damen, and J. F. Scott, in *Light Scattering Spectra of Solids*, edited by G. B. Wright (Springer-Verlag, New York, 1969), p. 359.

[4]M. V. Klein and S. P. S. Porto, Phys. Rev. Lett. **22,** 782 (1969).

[5]R. C. C. Leite, J. F. Scott, and T. C. Damen, Phys. Rev. Lett. **22,** 780 (1969).

[6]J. M. Ralston, R. L. Wadsack, and R. K. Chang, Phys. Rev. Lett. **25,** 814 (1970).

[7]T. C. Damen and J. F. Scott, Solid State Commun. **9,** 383 (1971).

[8]T. C. Damen and J. Shah, Phys. Rev. Lett. **27,** 1506 (1971).

[9]R. F. Williams and S. P. S. Porto, in *Light Scattering in Solids*, edited by M. Balkanski (Flammarion, Paris, 1971), p. 70.

[10]M. V. Klein and P. J. Colwell, in Ref. 9, p. 65.

[11]Y. Oka and T. Kushida, J. Phys. Soc. Japan (to be published).

[12]R. Loudon, Proc. R. Soc. A **275,** 218 (1963).

[13]A. K. Ganguly and J. L. Birman, Phys. Rev. **162,** 806 (1967).

[14]D. C. Hamilton, Phys. Rev. **188,** 1221 (1969).

[15]D. L. Mills and E. Burstein, Phys. Rev. **188,** 1465 (1969).

[16]E. Burstein, D. L. Mills, A. Pinczuk, and S. Ushioda, Phys. Rev. Lett. **22,** 348 (1969).

[17]B. Bendow and J. L. Birman, Phys. Rev. B **1,** 1678 (1970).

[18]B. Bendow, Phys. Rev. B **2,** 5051 (1970).

[19]E. Mulazzi, Phys. Rev. Lett. **25,** 228 (1970).

[20]M. L. Williams and J. Smit, Solid State Commun. **8,** 2009 (1970).

[21]B. Bendow, J. L. Birman, A. K. Ganguly, T. C. Damen, R. C. C. Leite, and J. F. Scott, Opt. Commun. **1,** 267 (1970).

[22]R. Martin, Phys. Rev. B **4,** 3676 (1971).

[23]R. M. Martin and T. C. Damen, Phys. Rev. Lett. **26,** 86 (1971).

[24]B. Bendow and J. L. Birman, in Ref. 9, p. 19.

[25]R. M. Martin, in Ref. 9, p. 25.

[26]R. M. Martin and C. M. Varmer, Phys. Rev. Lett. **26,** 1241 (1971).

[27]B. Bendow, Phys. Rev. B **4,** 552 (1971).

[28]R. Zeyher and C. S. Ting (unpublished).

[29]P. J. Colwell and M. V. Klein, Solid State Commun. **8,** 2095 (1970).

[30]J. O. Dimmock, in *II-VI Semiconducting Compounds*, edited by D. G. Thomas (Benjamin, New York, 1967), p. 277.

[31]J. F. Scott, T. C. Damen, W. T. Silfvast, R. C. C. Leite, and L. E. Chessman, Opt. Commun. **1,** 397 (1970).

[32]R. H. Callender, M. Balkanski, and J. L. Birman, in Ref. 9 p. 40.

[33]J. L. Lewis, R. L. Wadsack and R. K. Chang, in Ref. 9, p. 41.

[34]I. P. Kaminow and W. D. Johnston, Phys. Rev. **160,** 519 (1967).

[35]G. D. Boyd and D. A. Kleinman, J. Appl. Phys. **39,** 359 (1968).

[36]F. G. Parsons and R. K. Chang, Opt. Commun. **3,** 173 (1971).

[37]R. C. Miller and W. A. Nordland, Phys. Rev. B **2,** 4896 (1970).

[38]C. Flytzanis and J. Ducuing, Phys. Rev. **178,** 1218 (1969).

[39]J. C. Phillips and J. A. Van Vechten, Phys. Rev. **183,** 709 (1969).

[40]B. F. Levine, Phys. Rev. Lett. **22,** 787 (1969).

[41]J. F. Scott, Phys. Rev. B **2,** 1209 (1970).

[42]R. Loudon, Adv. Phys. **13,** 423 (1964).

[43]D. Dutton, Phys. Rev. **112,** 788 (1958).

[44]E. Gutsche, and J. Voigt, in Ref. 30, p. 337.

[44]H. Gobrecht and A. Bartschat, Z. Phys. **156,** 131 (1959).
[46]D. G. Thomas and J. J. Hopfield, Phys. Rev. **116,** 573 (1959).
[47]F. A. Jenkins and H. E. White, *Fundamentals of Optics*, 3rd ed. (McGraw-Hill, New York, 1957), p. 509ff, for example.
[48]C. A. Arguello, D. L. Rousseau, and S. P. S. Porto, Phys. Rev. **181,** 1351 (1969).
[49]A. D. Yoffe (private communication).
[50]D. G. Thomas, J. Phys. Chem. Solids **15,** 86 (1960).
[51]R. Loudon, in Ref. 3, p. 25.
[52]S. Ushioda, A. Pinczuk, W. Taylor, and E. Burstein, in Ref.30, p. 1185.
[53]S. Ushioda, A. Pinczuk, E. Burstein, and D. L. Mills, in Ref.3, p. 43.
[54]J. F. Scott, T. C. Damen, and J. Shah, Opt. Commun. **3,** 384 (1971).
[55]The determination of the sign and magnitude of γ requires a polariton scattering experiment. However, for γ_{xxz} in ZnO, a measurement of S_L/S_T is sufficient since this ratio was found to be essentially zero.
[56]Although the d coefficients were measured with incident radiation at 1.17 eV (1.064 μ), the signs are not expected to change for photon energies above the lattice modes and below the electronic transitions.
[57]M. A. Nusimovici, M. Balkanski, and J. L. Birman, Phys. Rev. B **1,** 595 (1970).
[58]B. F. Levine, Phys. Rev. Lett. **25,** 440 (1970).
[59]W. Y. Liang and A. D. Yoffe, Phys. Rev. Lett. **20,** 59 (1968).
[60]J. L. Birman (private communication).
[61]R. Zeyher (private communication).
[62]W. Richter, J. Phys. Chem. Solids (to be published).

PHYSICAL REVIEW B VOLUME 7, NUMBER 8 15 APRIL 1973

Perturbation-Theory Investigation of the Exciton Ground State of Cubic Semiconductors in a Magnetic Field

M. Altarelli*
Department of Physics and Astronomy, University of Rochester, Rochester, New York 14627

Nunzio O. Lipari
Xerox Corporation, Rochester Research Center, Webster, New York 14580

(Received 30 October 1972)

The influence of the degeneracy and anisotropy of the valence band on the exciton ground state in the low-magnetic-field region is investigated. Using first- and second-order perturbation theory, simple analytical expressions are given for the Zeeman splittings and the diamagnetic shifts of the eightfold-degenerate ground state. Selections rules for optical transitions and their dependence on polarization are discussed. The results are compared with available experimental data.

I. INTRODUCTION

The relevance of excitonic transitions in the interpretation of magneto-optical experiments has long been recognized.[1] From the theoretical point of view, the problem of the exciton in a magnetic field presents great difficulties, owing to the complexity of the valence-band structure in cubic semiconductors. So far, all investigations either have neglected the electron-hole interaction while retaining the complexity of the band structure,[2] or have treated the Coulomb interaction assuming simple parabolic bands.[3] The experimental results, however, show deviations from the predictions of these simplified approaches,[4-7] thus pointing out the need for a more accurate theory.[8]

The purpose of the present work is to investigate the lowest direct exciton states of diamond and zinc-blende semiconductors in the low-field region, taking into account both the Coulomb interaction and the actual band structure near the fundamental edge. In fact, it has been recently shown[9] that, in the absence of magnetic fields, the effects of the degeneracy and anisotropy of the valence band can be treated quite accurately. In the following we will show that it is also possible to include the effects of a weak magnetic field by similar methods.

In Sec. II the problem is formulated and the solution is presented. In Sec. III the results are discussed and compared with available experimental data.

II. PERTURBATION ANALYSIS

If we assume the conduction and valence-band extrema to be at the Γ point, we can write the Hamiltonian for the relative electron-hole motion in a magnetic field as[10]

$$\mathcal{H}_{ex} = \mathcal{H}_e\left(\vec{p} + \frac{e}{c}\vec{A}\right) - \mathcal{H}_h\left(-\vec{p} + \frac{e}{c}\vec{A}\right) - \frac{e^2}{\epsilon r}, \tag{1}$$

where, following Luttinger,[11] we have defined

$$\mathcal{H}_e(\vec{k}) = (1/2m_e^*)\,k^2 + \mu^*\,\vec{\sigma}\cdot\vec{H}, \tag{2}$$

$$-\mathcal{H}_h(\vec{k}) = (1/m_0)[(\gamma_1 + \tfrac{5}{2}\gamma_2)\tfrac{1}{2}k^2 - \gamma_2(k_x^2 J_x^2 + k_y^2 J_y^2 + k_z^2 J_z^2)$$